

High-Throughput Phenotyping of Clinical Text Using Large Language Models

Daniel B. Hier, S. Ilyas Munzir, Anne Stahlfeld, Tayo Obafemi-Ajayi, and Michael D. Carrithers

Abstract—High-throughput phenotyping automates the mapping of patient signs to standardized ontology concepts and is essential for precision medicine. This study evaluates the automation of phenotyping of clinical summaries from the Online Mendelian Inheritance in Man (OMIM) database using large language models. Due to their rich phenotype data, these summaries can be surrogates for physician notes. We conduct a performance comparison of GPT-4 and GPT-3.5-Turbo. Our results indicate that GPT-4 surpasses GPT-3.5-Turbo in identifying, categorizing, and normalizing signs, achieving concordance with manual annotators comparable to inter-rater agreement. Despite some limitations in sign normalization, the extensive pre-training of GPT-4 results in high performance and generalizability across several phenotyping tasks while obviating the need for manually annotated training data. Large language models are expected to be the dominant method for automating high-throughput phenotyping of clinical text.

Index Terms—phenotype, large language model, natural language processing, high-throughput, OMIM, neurology, HPO, GPT-4

I. INTRODUCTION

MANUAL phenotyping of electronic health records is laborious [1], [2]. Precision medicine has intensified the need for high-throughput methods to support the acquisition and processing of vast volumes of unstructured medical-related data [3], [4]. High-throughput phenotyping remains challenging due to the complexity of the task and the volume of physician notes [5]–[7]. Natural language processing (NLP) methods for identifying signs (concept recognition) in clinical text have evolved from rule-based and dictionary-based systems [8], [9], to machine learning and statistical models [10], [11], to deep learning methods such as recurrent neural networks (RNNs) and convolutional neural networks (CNNs) [12]–[15], and more recently to transformer architectures [16]–[21]. Barriers to the wider application of NLP methods to high-throughput phenotyping include limited accuracy, the need for large quantities of manually annotated data for training, and an inability to generalize an application from one domain of interest to another [2], [6], [7], [22].

Daniel B. Hier (email: dhier@uic.edu), Syed Ilyas Munzir (email: smunz2@uic.edu), Anne Stahlfeld (email: astahl5@uic.edu), and Michael D. Carrithers (email: mcarl@uic.edu) are with the University of Illinois at Chicago, Chicago IL 60612.

Tayo Obafemi-Ajayi is with the Engineering Program at Missouri State University, Springfield MO 65897 (email: tayooabafemijayai@missouristate.edu).

No protected health information was used in this research.

Python code and data files are available at the project GitHub site <https://github.com/clslabMSU/highthroughput-phenotyping>.

OMIM[®] and Online Mendelian Inheritance in Man[®] are registered trademarks of the Johns Hopkins University.

The emergence of large language models (LLMs) offers an opportunity to address previously unsolvable NLP problems, including the high-throughput phenotyping of physician notes [23]–[25]. LLMs belong to a class of foundation models which are inherently strong learners of heterogeneous data due to their large capacity, unified input modeling of different modalities, and improved multi-modal learning techniques [26]. LLMs have a superior ability to extract, summarize, translate, and generate textual information with only a few or even no prompt/fine-tuning samples [26]. Thus, they have been shown to perform well in high-throughput phenotyping [27] as they offer scalability and generalizability and require minimal additional training. Recent work in [28], [29] demonstrates their usefulness in processing large volumes of text in electronic health records (EHR) [28], [29]. They are also able to derive phenotypes from other text sources, such as PubMed abstracts and clinical summaries [27].

A goal of the precision medicine initiative is to use patient phenotypes to guide treatments and improve outcomes [30]. Patient phenotypes must be computable before being entered into precision medicine machine learning models. Patient phenotypes are recorded in EHRs as unstructured text. The most widely used standard for recording phenotypes is Human Phenotype Ontology (HPO) [1], [31], [32]. In a medical setting, the patient reports symptoms to the physician, who then examines the patient to obtain clinical signs. Together, these signs and symptoms constitute the phenotype of the patient. For brevity, we will collectively refer to these signs and symptoms as simply *signs*. The usual signs of the disease are the phenotypes of the disease. Online Mendelian Inheritance in Man (OMIM) provides a view of genetic heterogeneity of similar phenotypes across the genome for related diseases. This is referred to as *phenotypic series* i.e. a collection of phenotypes (diseases or traits) that are caused by mutations in different genes but have similar clinical features. For example, in OMIM, dystonia phenotypic series include several types of dystonia with different genetic causes such as DYT6, DYT11, and DYT25 [33], [34]. Each type of dystonia in this phenotypic series has similar clinical features, such as involuntary muscle contractions and abnormal postures but differ in their genetic causes based on mutations in different genes (e.g., TOR1A, THAP1, SGCE, GNAL). The phenotypic series in OMIM helps to categorize and understand the genetic heterogeneity of multiple diseases aiding in diagnosis and treatment strategies.

Patient phenotyping involves multiple steps, including sign identification (finding the sign in the text), sign categorization (assigning signs to high-level categories), sign normalization (mapping signs to terms in an ontology), and sign binarization

and vectorization. Sign categorization plays a crucial role in model interpretability and performance. For example, HPO currently has 17,957 terms descended from the root term *phenotypic abnormality*. Given this complexity, feature reduction is necessary to make phenotypes interpretable [35]–[38]. One approach (which we adopt in this work) to feature reduction of phenotypes is to ‘roll-up’ many granular terms into a small number of high-level categories [39].

The goal of this project is to perform automated high-throughput phenotyping on OMIM clinical summaries as a surrogate for the phenotyping of physician notes. This use case has advantages in that the text is easily available via an application programming interface (API), is rich in phenotypes and not protected by health privacy laws. Moreover, the task is similar to the phenotyping of physician notes [29]. The operational requirements of high-throughput phenotyping applied to healthcare include high processing speed, high accuracy, scalability to large data volumes, generalizability to various diseases, maintenance of privacy, and resilience to imperfect data inputs. The functional requirements of such a system include the ability to identify signs in free text, assign signs to high-level categories, map (normalize) signs to concepts in a designated ontology, and vectorize signs for use in computational models. This work evaluates the capabilities of two LLMs (GPT-4 and GPT-3.5-Turbo) in identifying, categorizing, and normalizing signs in clinical narratives. As a proof of concept, we vectorized phenotype data obtained from OMIM to visualize neurological disease variability within a phenotypic series with heatmaps as well as distances between different phenotypic series with dimension-reduced scatter plots.

II. DATA

The neurological disease and phenotypic data was retrieved from the OMIM database via their API (api.omim.org). Disease phenotypes are described in the *clinical synopsis* and the *clinical features* sections for each disease within the OMIM database. The *clinical synopsis* is a list of signs, symptoms, mode of inheritance, and age of onset. The *clinical features* section summarizes the published literature that underpins the phenotype of each disease. The OMIM API has separate calls for clinical features and clinical synopsis. The text from OMIM served as a surrogate for text from physician notes. Diseases in OMIM with similar phenotypes are grouped in a phenotypic series. OMIM currently has 582 Phenotypic Series, each with an identifier beginning with PS. We evaluated 16 phenotypic series that spanned across 405 neurogenetic diseases (see Table I).

III. METHODS

The high-throughput phenotyping pipeline extracts phenotypic terms in clinical text through the following steps (Fig. 1). Parameter details for the OMIM API and Open AI API calls are available on the project GitHub site.

Text Extraction and Preprocessing. Given a list of diseases and MIM numbers for each phenotypic series, the model

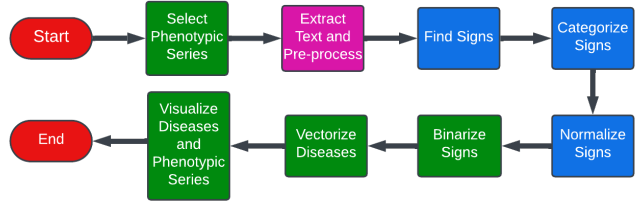


Fig. 1. **Pipeline for high-throughput phenotyping of clinical summaries from OMIM.** To support high-throughput, text retrieval, sign identification, sign categorization, and sign normalization is performed by an API.

TABLE I
PHENOTYPIC SERIES PROCESSED BY HIGH-THROUGHPUT PHENOTYPING

| Phenotypic Series | PS MIM | Diseases |
|--------------------------------------|----------|----------|
| amyotrophic lateral sclerosis (ALS) | PS105400 | 35 |
| Charcot-Marie-Tooth disease (CMT) | PS118220 | 81 |
| dystonia | PS128100 | 37 |
| epilepsy generalized | PS600669 | 29 |
| episodic ataxia | PS160120 | 9 |
| familial febrile seizures | PS121210 | 17 |
| hereditary spastic paraparesis (HSP) | PS303350 | 83 |
| hyperekplexia | PS149400 | 4 |
| leukodystrophy, hypomyelinating | PS312080 | 27 |
| narcolepsy | PS161400 | 7 |
| nemaline myopathy | PS161800 | 13 |
| Parkinson | PS168600 | 33 |
| progressive supranuclear palsy | PS601104 | 3 |
| restless legs | PS102300 | 8 |
| spinocerebellar ataxia | PS105400 | 40 |
| striato nigral degeneration | PS609161 | 2 |

reads and extracts clinical summaries from the OMIM API. (Parameter details are described on the project GitHub site.) White spaces and tabs were converted to a single white space. Commas, hyphens, semicolons, single quotes, double quotes, forward slashes, and backslashes were converted to a single white space. Periods were retained to identify sentence boundaries. The *Clinical Features* and *Description* sections from OMIM were normalized for further analysis.

Sign Identification. The aim is to identify neurological signs in the preprocessed text using the OpenAI API using the LLM. Text was passed to the OpenAI API with instructions to find all the signs within the text (Box 1).

Box 1: Prompt for Sign Identification

You are a neurologist analyzing a case summary from OMIM. Your input is text containing ‘Clinical Features’ and ‘Description’. Extract relevant neurological symptoms (patient complaints) and signs (findings on examination). Here’s how the output should look:

‘Signs’: [‘symptom a’, ‘symptom b’, ‘symptom c’]

Sign Categorization. The OpenAI API was given a list of identified signs with instructions to categorize them into one of 30 high-level categories (Box 2).

Sign Normalization. Signs were normalized by mapping them to the HPO using two approaches: the deep learning method combined spaCy (Explosion AI, Berlin) with Gensim BioWordVec embeddings. Vectors were generated for each sign and compared to vectorized HPO terms using cosine similarity. The HPO term with the highest cosine similarity to the retrieved sign was assigned as the best match. The LLM method involved passing a list of signs to GPT-4 or GPT-3.5-Turbo with instructions to map the sign to a term and ID in the HPO (Box 3).

Box 2: Prompt for Sign Categorization

You are a neurologist analyzing a list of signs. Classify each sign into one of these categories:

‘Behavior,’ ‘Bowel and Bladder,’ ‘Cognitive,’ ‘Deformity,’ ‘Dysautonomia,’ ‘Dystonia,’ ‘Extraocular Movements,’ ‘Fatigue,’ ‘Gait,’ ‘Head Shape,’ ‘Hearing,’ ‘Hyperkinesia,’ ‘Hyperreflexia,’ ‘Hypertonia,’ ‘Hypokinesia,’ ‘Hyporeflexia,’ ‘Hypotonia,’ ‘Incoordination,’ ‘Muscle Atrophy,’ ‘Other Cranial Nerve,’ ‘Pain,’ ‘Seizure,’ ‘Sensory,’ ‘Skin,’ ‘Sleep,’ ‘Speech,’ ‘Tremor,’ ‘Unclassified,’ ‘Vision,’ ‘Weakness.’

Your output should be a JSON object with each category as a key and a list of signs in that category as items.

Box 3: Prompt for Sign Normalization

You are a neurologist tasked with mapping each sign to a concept in the Human Phenotype Ontology (HPO). Your output should be a JSON object with each input sign as a key and two item values: the ‘HPO Term’ and the ‘HPO ID.’

For example:

```
{‘input’: ‘Apraxia oral,’
‘HPO Term’: ‘Oromotor apraxia,’
‘HPO ID’: ‘HP:0000687’ }
```

If the input term cannot be mapped to HPO, return ‘not-mappable’ in the ‘HPO Term’ and ‘HPO ID’ fields.

Category Binarization. Categories were binarized as either ‘0’ (no signs found in that category) or ‘1’ (one or more signs found in that category). If a disease had two or more terms in a phenotype category, such as ‘areflexia’ and ‘decreased reflexes’ in the *hyporeflexia* category, the category was scored as ‘1’, indicating one or more signs. The high-level categories are shown in Box 2.

Disease Vectorization. For each disease, a vector was assembled from the 30 binary phenotype categories so that the disease vector had 30 elements, each with a value of ‘0’ or ‘1’. Of the 405 diseases evaluated, 283 had adequate clinical

summaries in OMIM to allow high-throughput phenotyping and the creation of a disease vector. The disease vectors were stored as a data frame.

Visualization of Disease Heterogeneity within a Phenotypic Series. We created a separate heatmap for each phenotypic series to visualize similarities and differences between diseases within a phenotypic series (Seaborn library [40]). Each row in the heatmap was a disease in the phenotypic series. Each column was one of the 30 binarized phenotype categories (red for ‘present’, blue for ‘absent’.)

Visualization of Distances between the Centroids of Phenotypic Series. The 30 phenotype categories were reduced to two dimensions by principal component analysis (PCA). PCA calculated the coordinates of each disease in the phenotypic series, which were then shown as markers on a scatter plot (Fig. 7). Using the enhanced explainability plot approach described in [41], we calculated centroids for each phenotypic series, as shown as an ‘X’ on the scatter plot. For interpretability, we limited centroids to five phenotypic series per scatter plot. Distances between phenotypic series centroids represented relative similarities between different series as computed by PCA using the phenotype vectors.

Performance Metrics. The disease processing rate, the sign identification rate, sign categorization rate, and sign normalization rate were based on 405 diseases, a corpus of 175,724 words, and 16 phenotypic series (Table I).

The metrics for sign identification, sign categorization, and sign normalization were calculated based on a validation dataset of 40 diseases selected from the Dystonia, Parkinson, Hereditary Spastic Paraparesis, and Charcot-Marie-Tooth phenotypic series. In the validation dataset, GPT-4 found 609 signs, and GPT-3.5-Turbo found 358 signs. Sign identification was assessed by comparing signs identified by GPT-3.5-Turbo and GPT-4 with those identified by two manual annotators using the Prodigy annotation tool (Explosion AI, Berlin). Annotation methods have previously been described [42]. Manual annotators received instructions similar to those given to GPT-4 and GPT-3.5-Turbo. Two sets of signs were created for each of the 40 diseases in the validation dataset. The first set of signs were those found by GPT-3.5-Turbo or GPT-4. The second set was those found by the two manual annotators. Measures of agreement between the manual annotators and the LLMs included the mean Jaccard Index for each pair of sets, the highest cosine text similarity index (based on the spaCy similarity method and the Gensim BioWordVec embeddings) averaged across all available signs from each set, and the number of weak matches’ (similarity of less than 0.80) in each set. For sign identification, a sign from the GPT-sign set with at least 0.80 similarity to a sign in the manual-annotator-sign set was rated as a true positive’. A sign in the GPT-sign set with less than 0.80 similarity to any sign in the manual-annotator-sign set was rated as a false positive’. A sign in the manual-annotator-sign set with no counterpart in the GPT-sign-set with at least 0.80 similarity was rated as a false negative’.

To evaluate sign categorization, a neurology domain expert manually reviewed GPT-4 and GPT-3.5-Turbo sign categorization for diseases for each classifiable sign in the validation dataset and rated them as correct’ (true positive) or incorrect’

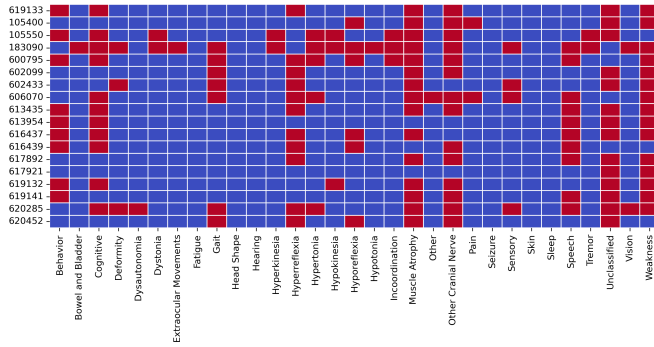


Fig. 2. **Heatmap for ALS phenotypic series with alphabetical category columns.** Diseases are along the y-axis. A unique MIM number identifies each disease. Compare to Fig. 3 with columns sorted by sign prevalence. Categories have been binarized so that ‘red’ indicates the phenotype was present, and ‘blue’ indicates the phenotype was absent.

(false negative). Signs considered uncategoryable by the domain expert were rated true negative’, whereas unclassifiable signs assigned a category by GPT-4 were rated false positives’. The expert also manually reviewed sign normalization using the SOTA NLP method, GPT-4, and GPT-3.5-Turbo.

For sign normalization to be rated as correct,’ both the normalized HPO term and the HPO ID had to be accurate. Signs that were considered unnormalizable by the domain expert were rated true negatives’. Unnormalizable signs normalized by GPT-4 were rated false positive.’ For normalizable signs, matching was rated as true positive’ or ‘false negative.’ Accuracy, precision, and recall were calculated using standard methods [43].

TABLE II
PERFORMANCE METRICS

| Model | GPT-3.5 Turbo | GPT-4 |
|--------------------------------|---------------|---------|
| Counts | | |
| Diseases | 405 | 405 |
| Usable Diseases | 207 | 283 |
| Signs Identified | 4,227 | 5,595 |
| Unique Signs Identified | 2,567 | 2,705 |
| Words Processed | 175,724 | 175,724 |
| Rates† | | |
| Disease Rate (sec/disease) | 14.2 | 16.4 |
| Identification Rate (sign/sec) | 5.7 | 4.2 |
| Categorization Rate (sign/sec) | 2.9 | 2.3 |
| Normalization Rate (sign/sec) | 9.3 | 9.3 |

† Performance times and rates are representative. They were obtained on Apple Mac Studio with an M2 ultra CPU running Mac OS 14.5.

IV. RESULTS

We performed high-throughput neurological phenotyping on 405 disease variants from 16 OMIM phenotypic series (Table I). Sign identification, sign categorization, and sign normalization were performed by GPT-3.5-Turbo or GPT-4 in three sequential submissions to the OpenAI API. GPT-3.5-Turbo and GPT-4 processing rates were 14.2 sec per disease and 16.4 sec per disease, respectively. Although higher

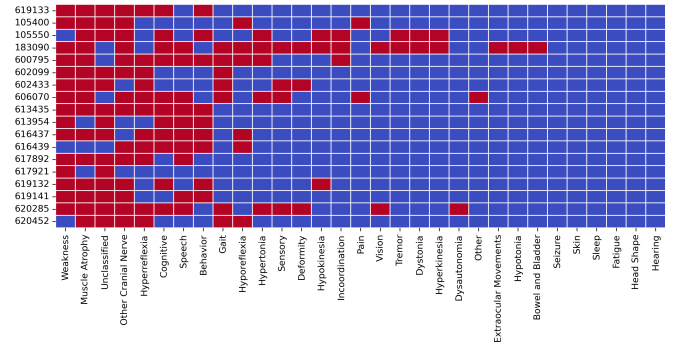


Fig. 3. **Heatmap for ALS phenotypic series with category columns sorted by sign prevalence** The most prevalent signs are weakness and muscle atrophy. Categories have been binarized so that ‘red’ indicates the phenotype was present and ‘blue’ indicates the phenotype was absent.

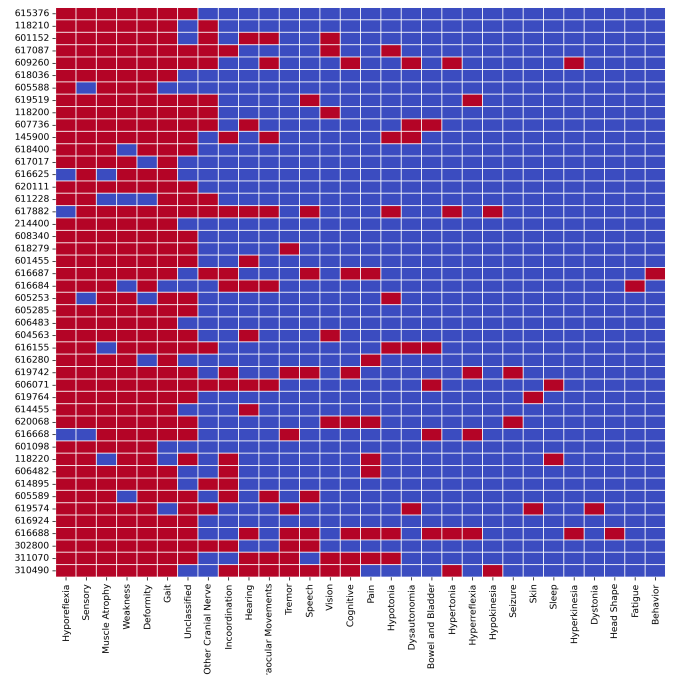


Fig. 4. **Heatmap for Charcot-Marie-Tooth phenotypic series.** The most prevalent signs are sensory symptoms, hyporeflexia, muscle atrophy, and weakness. MIM numbers for each disease in the phenotypic series are shown along the y-axis. Each row is a separate disease within the phenotypic series and illustrates the diversity of phenotypic presentations of CMT within the phenotypic series. Categories have been binarized so that ‘red’ indicates the phenotype was present and ‘blue’ indicates the phenotype was absent.

throughput might be possible with a faster CPU, more than 90% of the time expended was due to the four API calls.

The GPT-4 model outperformed the GPT-3.5-Turbo model on several performance metrics (Table II). GPT-4 produced usable data for 283 diseases, whereas GPT-3.5-Turbo produced usable data for 207 diseases. GPT-4 identified more signs (5,595 compared to 4,227) and more unique signs (2,705 compared to 2,567) than GPT-3.5-Turbo. The Jaccard Index, a stringent measure of concordance requiring exact matches between the large language models and the manual annotators, was higher for GPT-4 (0.31) than GPT-3.5-Turbo (0.16).

A more relaxed measure of concordance, the maximum



Fig. 5. **Word cloud for phenotypic terms for Charcot-Marie-Tooth disease phenotypic series.** 939 Terms were identified through GPT-4 API. Term size reflects relative frequency. Note that many similar terms include ‘areflexia’, ‘hyporeflexia’, and ‘decreased or absent reflexes’. Compare to Fig. 5 after terms have been further categorized by GPT-4 API.

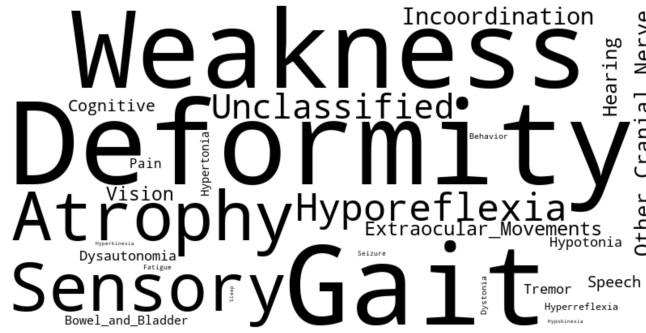


Fig. 6. **Word cloud for category frequencies for Charcot-Marie-Tooth (MCT) disease phenotypic series.** Phenotypic terms used to describe CMT diseases have been reduced to 30 categories. Word size in the word cloud reflects the size of each category. Compare to Fig. 4. The largest categories are Weakness, Deformity, and Gait.

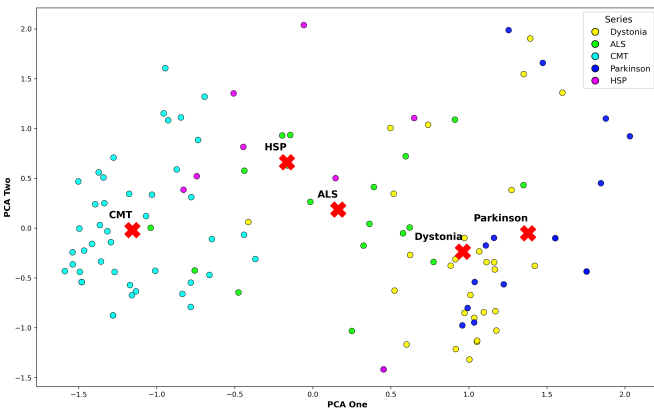


Fig. 7. **Centroids plotted by phenotypic series.** The feature space has been reduced from 30 high-level categories to 2 dimensions by PCA. Each round marker is a disease in one of the five plotted phenotypic series. The X indicates the centroids for each phenotypic series. The expected proximities between ALS and HSP (both with weakness and spasticity) and between Parkinson and Dystonia (both movement disorders) are visualized. Five of the 16 available phenotypic series centroids are shown. Creating centroid plots for any combinations of the phenotypic series in Table 1 is possible. Due to concerns about interpretability, we have limited centroid plots to no more than 5 phenotypic series per plot.

similarity index (based on cosine similarity from spaCy and BioWordVec embeddings from Gensim), showed high maximal mean similarities for signs compared to manual annotators (93.1 for GPT-3.5-Turbo and 94.2 for GPT-4). ‘Weak’ matches (maximum similarity less than 0.80) were lower with GPT-4 than with GPT-3.5-Turbo. Compared to manual annotators, precision, recall, and F1 for sign identification were higher with GPT-4 than with GPT-3.5.

The OpenAI API interface assigned each sign to one of 30 high-level categories. A significant simplification of the feature space was achieved by categorization of signs, as illustrated by comparing the word clouds for CMT signs (Fig.5 with CMT categories (Fig. 5). The ability of GPT-3.5-Turbo and GPT-4 to correctly assign signs to high-level categories was manually checked by a neurology expert for signs in the disease validation set. The accuracy of the GPT-4 was higher than that of the GPT-3.5-Turbo on sign categorization (94.0% compared to 58.4%). Sign categorization allowed us to create heatmaps for each phenotypic series where rows were diseases and columns were phenotype categories as illustrated by Figs. 2 to Fig. 4. Distances between phenotypic series centroids can be plotted using PCA for dimension reduction. Fig. 7 shows an example of five phenotypic series centroids.

Sign normalization was evaluated for the disease validation set. The SOTA NLP method performed best at 90.6% accuracy, followed by GPT-4 at 57.9% accuracy, and GPT-3.5-Turbo at 44.8% accuracy.

V. DISCUSSION

We have developed a high-throughput pipeline that processes clinical text and identifies signs of disease. To support high-throughput, ease of use, and processing speed, the pipeline uses application programming interfaces (APIs) [44]. We used an API to retrieve summary text from OMIM and another API to allow GPT-4 to identify, categorize, and normalize signs. Clinical summaries from the OMIM database were utilized as our use case since the text is easily retrievable, rich with phenotypes, and not regulated as protected health information. However, these methods can be applied to text from other sources, including electronic health records, PubMed abstracts, full-text articles, and other clinical summaries. This work involved ‘deep phenotyping,’ which can be distinguished from other work on ‘surface phenotyping.’ In deep phenotyping, the granular signs of disease are identified and mapped to an ontology [1]. Surface phenotyping is a less exacting process that assigns disease codes such as International Classification of Diseases (ICD) to physician notes or other clinical text [7], [15], [45], [46].

Recognizing (identifying signs) and normalizing (mapping signs to an ontology) are challenging tasks for traditional NLP methods [2], [22], [46]–[49]. Progress has been made toward improving the recognition and normalization of medical concepts using transformers combined with specialized biomedical word embeddings [20], [21]. Large pre-trained language models provide a new approach to deep phenotyping (concept identification and normalization) that does not require additional training or a large corpus of manual annotations

[27], [50]–[52]. Our pipeline for high-throughput phenotyping performed three phenotyping operations: sign identification, sign categorization, and sign normalization. In general, GPT-4 performed these operations with high accuracy and outperformed GPT-3.5-Turbo (Tables III, and IV).

TABLE III
SIGN IDENTIFICATION METRICS

| Model | GPT-3.5-Turbo* | GPT-4* | Inter-Rater** |
|----------------------|----------------|--------|---------------|
| Signs Identified | 358 | 609 | 694 |
| Weak Matches (%) | 15.0 | 11.6 | 4.0 |
| Jaccard Index | 0.16 | 0.35 | 0.36 |
| Max Similarity Index | 93.1 | 94.2 | 96.7 |
| F1 | 0.52 | 0.66 | 0.60 |
| Precision | 0.61 | 0.66 | 0.96 |
| Recall | 0.45 | 0.65 | 0.44 |

*Concordance for sign identification between GPT-3.5-Turbo and GPT-4 with the two manual annotators for 40 diseases in the validation dataset.

**Inter-rater concordance for the manual annotators. Note that GPT-4 achieves a Jaccard Index similar to that between manual annotators.

TABLE IV
SIGN CATEGORIZATION & NORMALIZATION

| Model | Accuracy | Precision | Recall |
|---------------|-----------|-----------|-----------|
| | C N | C N | C N |
| GPT-4 | 94.0 57.9 | 98.3 59.0 | 95.5 94.1 |
| GPT-3.5 Turbo | 58.4 44.8 | 78.4 49.8 | 95.2 52.9 |
| SOTA NLP | - 90.6 | - 90.8 | - 99.8 |

Metrics based on manual review of the categorization (C) and normalization (N) of signs of the 40 diseases in the validation dataset.

SOTA NLP is the spaCy cosine similarity method with Gensim BioWordVec embeddings.

Similarly, Groza et al. [27] evaluated GPT models for phenotype concept recognition using the ChatGPT interface. Their study demonstrated that GPT-4 outpaced state-of-the-art methods in mention-level F1 scores of 0.7. Our work extends that of Groza et al. by demonstrating the utility of the GPT API to facilitate high-throughput phenotyping. In previous work, we have shown that GPT-4 can identify phenotypes in physician notes [28], [29], which is important for precision medicine [53], [54].

GPT-4 exhibited some weaknesses in sign normalization, achieving an accuracy of only 57.9%. This task has been noted by others as particularly challenging for GPT-4 [27]. In comparison, a state-of-the-art (SOTA) NLP model that combined BioWordVec from Gensim with the spaCy NLP similarity method demonstrated significantly higher accuracy at 90.6%. While GPT-4 excelled at identifying plausible HPO terms for each input term, it was notably less accurate in providing the correct HPO IDs. In some instances, it even produced implausible HPO IDs. This discrepancy likely stems from GPT-4’s design, which relies heavily on pre-training to infer HPO IDs rather than employing a direct lookup capability. Currently, GPT-4 does not have an inherent mechanism to verify or retrieve accurate HPO IDs from a database.

Moreover, an inherent limitation of GPT models like GPT-4 is their non-deterministic nature. The choice of HPO ID for sign normalization can vary between different runs, even when the same input is provided [27]. This variability introduces inconsistencies that can be problematic in clinical applications where precision and reliability are paramount. Despite these limitations, GPT-4’s ability to generate plausible HPO terms highlights its potential for improvement with enhancements such as integrating a lookup mechanism for HPO IDs or using hybrid models that combine the strengths of GPT-4 with deterministic systems like BioWordVec and spaCy.

We used GPT-4 to categorize the signs into 30 high-level categories. These high-level categories were chosen for their relevance to neurological phenotypes [55]. Although HPO has 28 high-level categories under *Phenotypic abnormality* [56], these categories are too broad to be useful in analyzing the phenotypes of neurological diseases. This categorization process significantly reduced the number of phenotypic terms needed to describe the diseases (compare Fig. 5 to Fig. 6). By assigning each phenotypic term to one of 30 high-level categories, we gained the ability to represent each disease in a phenotypic series as a row on a heatmap (Figs. 2 to 4). Heatmaps have also been used to visualize Orphadata disease phenotypes [55].

Once the phenotypic terms are acquired, a disease phenotype can be represented as a vector. Various methods to calculate similarity between these disease vectors are available [35], [37], [57]–[60]. We used Principal Component Analysis (PCA) to reduce the dimensionality of these vectors to two dimensions (x and y), enabling us to visualize each disease as a marker on a scatter plot. To visualize distances between the phenotypic series, we represented each series as a centroid of its component diseases. Although Fig. 7 is representative, these methods can be applied to display phenotypic distances between any combination of diseases or phenotypic series.

Large language models, including GPT-4, show promise for high-throughput phenotyping of clinical text though some issues identified in this work warrant further investigation. The level of accuracy required by LLMs for clinical decision-making remains uncertain [61]. It is important to recognize that human annotators do not always agree perfectly [42], and even expert physicians are susceptible to diagnostic errors [62]. There is ongoing debate over whether health informatics tasks, such as phenotyping, are better suited to large general-purpose models or smaller, specially trained language models [63]. Concerns have been raised about the foundational weaknesses of large language models in healthcare, stemming from their limited training on EHR data [64]. Additionally, LLMs often struggle to process EHR data in tabular form (e.g., long tables of biochemical results found in EHRs) [65]. Groza et al. [27] have highlighted the stochastic nature of LLM outputs. If these models are to be used routinely in healthcare, issues of trust, privacy, equity, fairness, and confidentiality must be satisfactorily addressed [66], [67]. Furthermore, the problem of ‘hallucinations’ and ‘confabulations’ by LLMs remains unresolved [68].

Future work will fully assess the robustness and error-handling capabilities of our pipeline. While we tested GPT-

3.5-Turbo and GPT-4, we did not compare their performance with other proprietary or open-source models. Scalability, cost analysis and stability studies are also required. Note that the neurological disease and phenotypic data utilized in this work were not protected health information, but privacy concerns must still be addressed.

Nonetheless, the case for applying large language models to high-throughput phenotyping is compelling [25], [27], [50]–[52], [69]–[71]. These models are fast, accurate, and ready to run ‘out of the box.’ Unlike traditional neural network models, they do not rely on an extensive corpus of manual annotations. These models should be generalizable to a variety of diseases without additional training. Current limitations in sign normalization can be addressed using techniques from augmented retrieval generation [72], by additional pre-training, or by creating small specialized models specifically for sign normalization. Large language models such as GPT-4 are expected to become the dominant method for high-throughput clinical text phenotyping.

REFERENCES

- [1] P. N. Robinson, “Deep phenotyping for precision medicine,” *Human mutation*, vol. 33, no. 5, pp. 777–780, 2012.
- [2] J. Pathak, A. N. Kho, and J. C. Denny, “Electronic health records-driven phenotyping: challenges, recent advances, and perspectives,” *Journal of the American Medical Informatics Association*, vol. 20, no. e2, pp. e206–e211, 2013.
- [3] M. Afzal, S. R. Islam, M. Hussain, and S. Lee, “Precision medicine informatics: principles, prospects, and challenges,” *IEEE Access*, vol. 8, pp. 13 593–13 612, 2020.
- [4] M. Sahu, R. Gupta, R. K. Ambasta, and P. Kumar, “Artificial intelligence and machine learning in precision medicine: A paradigm shift in big data analysis,” *Progress in Molecular Biology and Translational Science*, vol. 190, no. 1, pp. 57–100, 2022.
- [5] S. Shivade, P. Raghavan, E. Fosler-Lussier, P. J. Embi, N. Elhadad, S. B. Johnson, and A. M. Lai, “A review of approaches to identifying patient phenotype cohorts using electronic health records,” *Journal of the American Medical Informatics Association*, vol. 21, no. 2, pp. 221–230, 2014.
- [6] Y. Chen, R. J. Carroll, E. R. M. Hinz, A. Shah, A. E. Eyler, J. C. Denny, and H. Xu, “Applying active learning to high-throughput phenotyping algorithms for electronic health records data,” *Journal of the American Medical Informatics Association*, vol. 20, no. e2, pp. e253–e259, 2013.
- [7] K. P. Liao, J. Sun, T. A. Cai, N. Link, C. Hong, J. Huang, J. E. Huffman, J. Gronsbell, Y. Zhang, Y.-L. Ho *et al.*, “High-throughput multimodal automated phenotyping (map) with application to phewas,” *Journal of the American Medical Informatics Association*, vol. 26, no. 11, pp. 1255–1262, 2019.
- [8] S. Eltyeb and N. Salim, “Chemical named entities recognition: a review on approaches and applications,” *Journal of cheminformatics*, vol. 6, no. 1, pp. 1–12, 2014.
- [9] A. P. Quimbaya, A. S. Múnera, R. A. G. Rivera, J. C. D. Rodríguez, O. M. M. Velandia, A. A. G. Peña, and C. Labbé, “Named entity recognition over electronic health records through a combined dictionary-based approach,” *Procedia Computer Science*, vol. 100, pp. 55–61, 2016.
- [10] L. Hirschman, A. A. Morgan, and A. S. Yeh, “Rutabaga by any other name: extracting biological names,” *Journal of Biomedical Informatics*, vol. 35, no. 4, pp. 247–259, 2002.
- [11] Ö. Uzuner, B. R. South, S. Shen, and S. L. DuVall, “2010 i2b2/va challenge on concepts, assertions, and relations in clinical text,” *Journal of the American Medical Informatics Association*, vol. 18, no. 5, pp. 552–556, 2011.
- [12] G. Lample, M. Ballesteros, S. Subramanian, K. Kawakami, and C. Dyer, “Neural architectures for named entity recognition,” *arXiv preprint arXiv:1603.01360*, 2016.
- [13] J. P. Chiu and E. Nichols, “Named entity recognition with bidirectional LSTM-CNNs,” *Transactions of the Association for Computational Linguistics*, vol. 4, pp. 357–370, 2016.
- [14] M. Habibi, L. Weber, M. Neves, D. L. Wiegandt, and U. Leser, “Deep learning with word embeddings improves biomedical named entity recognition,” *Bioinformatics*, vol. 33, no. 14, pp. i37–i48, 2017.
- [15] S. Gehrmann, F. Dernoncourt, Y. Li, E. T. Carlson, J. T. Wu, J. Welt, J. Foote Jr, E. T. Moseley, D. W. Grant, P. D. Tyler *et al.*, “Comparing deep learning and concept extraction based methods for patient phenotyping from clinical narratives,” *PLoS one*, vol. 13, no. 2, p. e0192360, 2018.
- [16] J. Devlin, M.-W. Chang, K. Lee, and K. Toutanova, “BERT: Pre-training of deep bidirectional transformers for language understanding,” *arXiv preprint arXiv:1810.04805*, 2018.
- [17] A. Vaswani, N. Shazeer, N. Parmar, J. Uszkoreit, L. Jones, A. N. Gomez, E. Kaiser, and I. Polosukhin, “Attention is all you need,” in *Advances in neural information processing systems*, 2017, pp. 5998–6008.
- [18] R. Zhu, X. Tu, and J. X. Huang, “Utilizing BERT for biomedical and clinical text mining,” in *Data Analytics in Biomedical Engineering and Healthcare*. Elsevier, 2021, pp. 73–103.
- [19] X. Yu, W. Hu, S. Lu, X. Sun, and Z. Yuan, “Biobert based named entity recognition in electronic medical record,” *2019 10th international conference on information technology in medicine and education (ITME)*, pp. 49–52, 2019.
- [20] J. Lee, W. Yoon, S. Kim, D. Kim, S. Kim, C. H. So, and J. Kang, “Biobert: a pre-trained biomedical language representation model for biomedical text mining,” *Bioinformatics*, vol. 36, no. 4, pp. 1234–1240, 2020.
- [21] Z. Ji, Q. Wei, and H. Xu, “Bert-based ranking for biomedical entity normalization,” *AMIA Summits on Translational Science Proceedings*, vol. 2020, p. 269, 2020.
- [22] H. Alzoubi, R. Alzubi, N. Ramzan, D. West, T. Al-Hadhrani, and M. Alazab, “A review of automatic phenotyping approaches using electronic health records,” *Electronics*, vol. 8, no. 11, p. 1235, 2019.
- [23] C. Yan, H. Ong, M. Grabowska, M. Krantz, W.-C. Su, A. Dickson, J. F. Peterson, Q. Feng, D. M. Roden, C. M. Stein *et al.*, “Large language models facilitate the generation of electronic health record phenotyping algorithms,” *medRxiv*, pp. 2023–12, 2023.
- [24] J. Yang, C. Liu, W. Deng, D. Wu, C. Weng, Y. Zhou, and K. Wang, “Enhancing phenotype recognition in clinical notes using large language models: Phenobert and phenogpt,” *Patterns*, 2023.
- [25] A. Wang, C. Liu, J. Yang, and C. Weng, “Fine-tuning large language models for rare disease concept normalization,” *bioRxiv*, pp. 2023–12, 2023.
- [26] J. Qiu, L. Li, J. Sun, J. Peng, P. Shi, R. Zhang, Y. Dong, K. Lam, F. P.-W. Lo, B. Xiao *et al.*, “Large ai models in health informatics: Applications, challenges, and the future,” *IEEE Journal of Biomedical and Health Informatics*, 2023.
- [27] T. Groza, H. Caufield, D. Gratton, G. Baynam, M. A. Haendel, P. N. Robinson, C. J. Mungall, and J. T. Reese, “An evaluation of gpt models for phenotype concept recognition,” *BMC Medical Informatics and Decision Making*, vol. 24, no. 1, p. 30, 2024.
- [28] S. I. Munzir, D. B. Hier, C. Oommen, and M. D. Carrithers, “A large language model outperforms other computational approaches to the high-throughput phenotyping of physician notes,” *arXiv preprint arXiv:2406.14757*, 2024, accepted in AMIA Annual Symposium 2024. [Online]. Available: <https://arxiv.org/abs/2406.14757>
- [29] S. I. Munzir, D. B. Hier, and M. D. Carrithers, “High throughput phenotyping of physician notes with large language and hybrid nlp models,” *arXiv preprint arXiv:2403.05920*, 2024, accepted in International Conference of the IEEE Engineering in Medicine & Biology Society (EMBC 2024). [Online]. Available: <https://doi.org/10.48550/arXiv.2403.05920>
- [30] J. P. Ackerman, D. C. Bartos, J. D. Kapplinger, D. J. Tester, B. P. Delisle, and M. J. Ackerman, “The promise and peril of precision medicine: phenotyping still matters most,” in *Mayo Clinic Proceedings*, vol. 91, no. 11. Elsevier, 2016, pp. 1606–1616.
- [31] J. S. Amberger, C. A. Bocchini, F. Schiettecatte, A. F. Scott, and A. Hamosh, “Omim.org: Online mendelian inheritance in man (omim®), an online catalog of human genes and genetic disorders,” *Nucleic acids research*, vol. 43, no. D1, pp. D789–D798, 2015.
- [32] S. Köhler, N. A. Vasilevsky, M. Engelstad, E. Foster, J. McMurry, S. Aymé, G. Baynam, S. M. Bello, C. F. Boerkoel, K. M. Boycott *et al.*, “The human phenotype ontology in 2017,” *Nucleic acids research*, vol. 45, no. D1, pp. D865–D876, 2017.
- [33] D. Hier, R. Yelugam, S. Azizi, and D. Wunsch III, “A focused review of deep phenotyping with examples from neurology,” *Eur Sci J*, vol. 18, pp. 4–19, 2022.

- [34] D. Hier, R. Yelugam, S. Azizi, M. Carrithers, and I. Wunsch, “Dc. high throughput neurological phenotyping with metamap,” *Eur Sci J*, vol. 18, pp. 37–49, 2022.
- [35] M. Chagoyen and F. Pazos, “Characterization of clinical signs in the human interactome,” *Bioinformatics*, vol. 32, no. 12, pp. 1761–1765, 2016.
- [36] L. Licata, A. Via, P. Turina, G. Babbi, S. Benevenuta, C. Carta, R. Casadio, A. Cicconardi, A. Facchiano, P. Fariselli *et al.*, “Resources and tools for rare disease variant interpretation,” *Frontiers in Molecular Biosciences*, vol. 10, p. 1169109, 2023.
- [37] L. Cheng, H. Zhao, P. Wang, W. Zhou, M. Luo, T. Li, J. Han, S. Liu, and Q. Jiang, “Computational methods for identifying similar diseases,” *Molecular Therapy-Nucleic Acids*, vol. 18, pp. 590–604, 2019.
- [38] J. Peng, H. Xue, Y. Shao, X. Shang, Y. Wang, and J. Chen, “A novel method to measure the semantic similarity of hpo terms,” *International Journal of Data Mining and Bioinformatics*, vol. 17, no. 2, pp. 173–188, 2017.
- [39] D. C. Wunsch III and D. B. Hier, “Subsumption reduces dataset dimensionality without decreasing performance of a machine learning classifier,” in *2021 43rd Annual International Conference of the IEEE Engineering in Medicine & Biology Society (EMBC)*. IEEE, 2021, pp. 1618–1621.
- [40] M. L. Waskom, “seaborn: statistical data visualization,” *Journal of Open Source Software*, vol. 6, no. 60, p. 3021, 2021. [Online]. Available: <https://doi.org/10.21105/joss.03021>
- [41] D. B. Hier, T. Obafemi-Ajayi, G. R. Olbricht, D. M. Burns, S. Petrenko, and D. C. Wunsch II, “Enhancing dimension-reduced scatter plots with class and feature centroids,” *arXiv preprint arXiv:2403.20246*, 2024.
- [42] C. Oommen, Q. Howlett-Prieto, M. D. Carrithers, and D. B. Hier, “Inter-rater agreement for the annotation of neurologic signs and symptoms in electronic health records,” *Frontiers in Digital Health*, vol. 5, p. 1075771, 2023.
- [43] D. M. Powers, “Evaluation: from precision, recall and f-measure to roc, informedness, markedness and correlation,” *arXiv preprint arXiv:2010.16061*, 2020.
- [44] A. Tarkowska, D. Carvalho-Silva, C. E. Cook, E. Turner, R. D. Finn, and A. D. Yates, “Eleven quick tips to build a usable rest api for life sciences,” *PLoS computational biology*, vol. 14, no. 12, p. e1006542, 2018.
- [45] M. A. Gehan and E. A. Kellogg, “High-throughput phenotyping,” *American journal of botany*, vol. 104, no. 4, pp. 505–508, 2017.
- [46] Y. Zhang, T. Cai, S. Yu, K. Cho, C. Hong, J. Sun, J. Huang, Y.-L. Ho, A. N. Ananthakrishnan, Z. Xia *et al.*, “High-throughput phenotyping with electronic medical record data using a common semi-supervised approach (phcap),” *Nature protocols*, vol. 14, no. 12, pp. 3426–3444, 2019.
- [47] S. Fu, D. Chen, H. He, S. Liu, S. Moon, K. J. Peterson, F. Shen, L. Wang, Y. Wang, A. Wen *et al.*, “Clinical concept extraction: a methodology review,” *Journal of Biomedical Informatics*, p. 103526, 2020.
- [48] M. Agrawal, C. O’Connell, Y. Fatemi, A. Levy, and D. Sontag, “Robust benchmarking for machine learning of clinical entity extraction,” in *Machine Learning for Healthcare Conference*. PMLR, 2020, pp. 928–949.
- [49] S. Yang, P. Varghese, E. Stephenson, K. Tu, and J. Gronsbell, “Machine learning approaches for electronic health records phenotyping: a methodical review,” *Journal of the American Medical Informatics Association*, vol. 30, no. 2, pp. 367–381, 2023.
- [50] C. Shyr, Y. Hu, P. A. Harris, and H. Xu, “Identifying and extracting rare disease phenotypes with large language models,” *arXiv preprint arXiv:2306.12656*, 2023.
- [51] C. Shyr, Y. Hu, L. Bastarache, A. Cheng, R. Hamid, P. Harris, and H. Xu, “Identifying and extracting rare diseases and their phenotypes with large language models,” *Journal of Healthcare Informatics Research*, pp. 1–24, 2024.
- [52] N. J. Dobbins, “Generalizable and scalable multistage biomedical concept normalization leveraging large language models,” *arXiv preprint arXiv:2405.15122*, 2024.
- [53] M. Simmons, A. Singhal, and Z. Lu, “Text mining for precision medicine: bringing structure to ehers and biomedical literature to understand genes and health,” *Translational Biomedical Informatics: A Precision Medicine Perspective*, pp. 139–166, 2016.
- [54] A. Sitapati, H. Kim, B. Berkovich, R. Marmor, S. Singh, R. El-Kareh, B. Clay, and L. Ohno-Machado, “Integrated precision medicine: the role of electronic health records in delivering personalized treatment,” *Wiley Interdisciplinary Reviews: Systems Biology and Medicine*, vol. 9, no. 3, p. e1378, 2017.
- [55] D. B. Hier, R. Yelugam, M. D. Carrithers, and D. C. Wunsch III, “The visualization of orphadata neurology phenotypes,” *Frontiers in Digital Health*, vol. 5, p. 1064936, 2023.
- [56] J. Foreman, S. Brent, D. Perrett, A. P. Bevan, S. E. Hunt, F. Cunningham, M. E. Hurles, and H. V. Firth, “Decipher: Supporting the interpretation and sharing of rare disease phenotype-linked variant data to advance diagnosis and research,” *Human Mutation*, vol. 43, no. 6, pp. 682–697, 2022.
- [57] T. Mabotuwana, M. C. Lee, and E. V. Cohen-Solal, “An ontology-based similarity measure for biomedical data—application to radiology reports,” *Journal of biomedical informatics*, vol. 46, no. 5, pp. 857–868, 2013.
- [58] A. Gamba, M. Salmona, L. Cantù, and G. Bazzoni, “The similarity of inherited diseases (ii): clinical and biological similarity between the phenotypic series,” *BMC Medical Genomics*, vol. 13, pp. 1–11, 2020.
- [59] A. Gamba, M. Salmona, and G. Bazzoni, “The similarity of inherited diseases (i): clinical similarity within the phenotypic series,” *BMC Medical Genomics*, vol. 14, pp. 1–12, 2021.
- [60] H. Xue, J. Peng, and X. Shang, “Predicting disease-related phenotypes using an integrated phenotype similarity measurement based on hpo,” *BMC systems biology*, vol. 13, pp. 1–12, 2019.
- [61] Z. Grotenhuis, “Text mining of clinical outcomes for medical research: how accurate should it be?” MSc. Thesis, Utrecht University, Utrecht, The Netherlands, October 2022.
- [62] M. I. Chimowitz, E. L. Logigian, and L. R. Caplan, “The accuracy of bedside neurological diagnoses,” *Annals of neurology*, vol. 28, no. 1, pp. 78–85, 1990.
- [63] E. Hernandez, D. Mahajan, J. Wulff, M. J. Smith, Z. Ziegler, D. Nadler, P. Szolovits, A. Johnson, E. Alsentzer *et al.*, “Do we still need clinical language models?” in *Conference on Health, Inference, and Learning*. PMLR, 2023, pp. 578–597.
- [64] M. Wornow, Y. Xu, R. Thapa, B. Patel, E. Steinberg, S. Fleming, M. A. Pfeffer, J. Fries, and N. H. Shah, “The shaky foundations of large language models and foundation models for electronic health records,” *npj Digital Medicine*, vol. 6, no. 1, p. 135, 2023.
- [65] J. Lovón-Melgarejo, T. Ben-Haddi, J. Di Scala, J. G. Moreno, and L. Tamine, “Revisiting the mimic-iv benchmark: Experiments using language models for electronic health records,” in *Proceedings of the First Workshop on Patient-Oriented Language Processing (CLHealth)@ LREC-COLING 2024*, 2024, pp. 189–196.
- [66] S. Harter, “Attention is not all you need: the complicated case of ethically using large language models in healthcare and medicine,” *EBioMedicine*, vol. 90, 2023.
- [67] L. Sun, Y. Huang, H. Wang, S. Wu, Q. Zhang, C. Gao, Y. Huang, W. Lyu, Y. Zhang, X. Li *et al.*, “Trustllm: Trustworthiness in large language models,” *arXiv preprint arXiv:2401.05561*, 2024.
- [68] I. S. Schwartz, K. E. Link, R. Daneshjou, and N. Cortés-Penfield, “Black box warning: large language models and the future of infectious diseases consultation,” *Clinical infectious diseases*, vol. 78, no. 4, pp. 860–866, 2024.
- [69] W. E. Thompson, D. M. Vidmar, J. K. De Freitas, J. M. Pfeifer, B. K. Fornwalt, R. Chen, G. Altay, K. Manghnani, A. C. Nelsen, K. Morland *et al.*, “Large language models with retrieval-augmented generation for zero-shot disease phenotyping,” *arXiv preprint arXiv:2312.06457*, 2023.
- [70] S. Kafkas, M. Abdelhakim, A. Althagafi, S. Toonsi, M. Alghamdi, P. N. Schofield, and R. Hoehndorf, “The application of large language models to the phenotype-based prioritization of causative genes in rare disease patients,” *medRxiv*, pp. 2023–11, 2023.
- [71] A. Wang, C. Liu, J. Yang, and C. Weng, “Fine-tuning large language models for rare disease concept normalization,” *Journal of the American Medical Informatics Association*, p. ocae133, 2024.
- [72] J. Chen, H. Lin, X. Han, and L. Sun, “Benchmarking large language models in retrieval-augmented generation,” in *Proceedings of the AAAI Conference on Artificial Intelligence*, vol. 38, no. 16, 2024, pp. 17754–17762.